

Sequential short-time propagation of quantum–classical dynamics

Donal MacKernan¹, Raymond Kapral² and Giovanni Ciccotti³

¹ CECAM, Ecole Normale Supérieure de Lyon, 46 Allée d'Italie, 69364 Lyon Cedex 07, France

² Chemical Physics Theory Group, Department of Chemistry, University of Toronto, Toronto, Ont., Canada M5S 3H6

³ INFN and Dipartimento di Fisica, Università 'La Sapienza', Piazzale Aldo Moro 2, 00185 Roma, Italy

Received 14 June 2002

Published 27 September 2002

Online at stacks.iop.org/JPhysCM/14/9069

Abstract

An algorithm for the simulation of quantum–classical dynamics is presented. Quantum–classical evolution is effected by a propagator $\exp(i\hat{\mathcal{L}}t)$ involving the quantum classical Liouville operator $\hat{\mathcal{L}}$ that describes the evolution of a quantum subsystem coupled to a classical bath. Such a mixed description provides a means to study the dynamics of complex many-body systems where certain degrees of freedom are treated quantum mechanically. The algorithm is constructed by decomposing the time interval t into small segments of length Δt and successively applying the propagator in the short time segments to obtain the evolution for long times. The algorithm is shown to be a discretization of the iterated Dyson form of the propagator whose direct solution is vexatious. The sequential short-time propagation algorithm is applied to the spin-boson model for a range of values of the Kondo parameter and shown to be effective.

1. Introduction

The dynamics of a many-body system may often be described in terms of mixed quantum–classical dynamics: certain relevant degrees of freedom which are treated quantum mechanically are coupled to a classical environment [1–3]. Such a description is especially useful for the study of the quantum dynamics of protonic and electronic degrees of freedom in condensed phase systems since the large number of environmental phase-space coordinates can be treated by classical mechanics. Although a mixed quantum–classical description is a major simplification of full quantum dynamics, quantum–classical dynamics is not simple since coupling between the quantum and classical subsystems precludes a Newtonian description of the bath [4]. Consequently, the development of methods to describe and simulate such quantum–classical dynamics is a problem of considerable interest. A number of approximate approaches has been developed in the past to follow the joint evolution of the classical and quantum subsystems [5–13]. The main question to be answered using these approaches is how

to compute the evolution of the classical part when quantum transitions occur. Another issue which must be addressed is how to compute the statistical properties of a quantum–classical system. In a recent series of papers we showed how one may formulate both the dynamics and statistical mechanics of quantum–classical systems by using a partial Wigner representation and taking the limit of a small mass ratio of the masses of the particles belonging to the quantum and classical subsystems [4, 12–14].

In our formulation of quantum–classical dynamics [4], observables or dynamical variables $\hat{B}_W(R, P)$ are operators in the quantum degrees of freedom and functions of the classical phase-space coordinates (R, P) of the bath. Dynamical variables satisfy the equation of motion

$$\frac{d\hat{B}_W(t)}{dt} = i\hat{\mathcal{L}}\hat{B}_W(t), \quad (1)$$

where $i\hat{\mathcal{L}} = (i/\hbar)[\hat{H}_W, \cdot] - (1/2)(\{\hat{H}_W, \cdot\} - \{\cdot, \hat{H}_W\})$ is the quantum–classical Liouville operator, with $\hat{H}_W(R, P) = P^2/2M + \hat{p}^2/2m + \hat{V}_W(\hat{q}, R) \equiv P^2/2M + \hat{h}_W(R)$ the partially Wigner transformed [15] Hamiltonian of the system. The quantum subsystem has position and momentum operators \hat{q} and \hat{p} , respectively. The potential energy operator $\hat{V}_W(\hat{q}, R)$ accounts for interactions among all particles, both quantum and classical. One can see that this evolution equation reduces to the familiar Heisenberg equation of motion if the bath is absent and to the classical Newtonian equations of motion (in Liouville form) if the quantum subsystem is absent. Due to the mutual interaction between these two subsystems, the evolution of the entire quantum–classical system given by equation (1) is more complex than the classical limit and, formally, more involved than quantum evolution. While the formal solution of this equation of motion is easily written as $\hat{B}_W(t) = \exp(i\hat{\mathcal{L}}t)\hat{B}_W(0)$, the problem is to design methods to effectively simulate the evolution for realistic many-body systems.

Quantum–classical dynamics described by the Liouville operator $i\hat{\mathcal{L}}$ may be formulated in terms of an ensemble of surface-hopping trajectories. For this purpose, it is convenient to work in a basis of adiabatic eigenfunctions $|\alpha; R\rangle$ determined from the solution of the eigenvalue problem, $\hat{h}_W(R)|\alpha; R\rangle = E_\alpha(R)|\alpha; R\rangle$. In this basis the quantum–classical Liouville operator has matrix elements [4]

$$i\mathcal{L}_{\alpha\alpha',\beta\beta'} = (i\omega_{\alpha\alpha'} + iL_{\alpha\alpha'})\delta_{\alpha\beta}\delta_{\alpha'\beta'} - J_{\alpha\alpha',\beta\beta'} \equiv i\mathcal{L}_{\alpha\alpha'}^0\delta_{\alpha\beta}\delta_{\alpha'\beta'} - J_{\alpha\alpha',\beta\beta'}, \quad (2)$$

where $\omega_{\alpha\alpha'} = (E_\alpha - E_{\alpha'})/\hbar$ is a frequency determined by the difference in energies of adiabatic states and $iL_{\alpha\alpha'}$ is the Liouville operator that describes classical evolution subjected to the mean of the Hellmann–Feynman forces for adiabatic states α and α' . The operator $J_{\alpha\alpha',\beta\beta'}$ is responsible for non-adiabatic transitions and corresponding variations with respect to the bath momentum, and has the form

$$J_{\alpha\alpha',\beta\beta'} = -\frac{P}{M}d_{\alpha\beta}\left(1 + \frac{1}{2}S_{\alpha\beta}\frac{\partial}{\partial P}\right)\delta_{\alpha'\beta'} - \frac{P}{M}d_{\alpha'\beta'}^*\left(1 + \frac{1}{2}S_{\alpha'\beta'}^*\frac{\partial}{\partial P}\right)\delta_{\alpha\beta}, \quad (3)$$

where $S_{\alpha\beta} = (E_\alpha - E_\beta)d_{\alpha\beta}(\frac{P}{M}d_{\alpha\beta})^{-1}$. A solution in terms of an ensemble of surface-hopping trajectories is easily constructed by writing the evolution operator as an integral equation of the Dyson form:

$$(e^{i\hat{\mathcal{L}}t})_{\alpha\alpha',\beta\beta'} = e^{i\mathcal{L}_{\alpha\alpha'}^0 t}\delta_{\alpha\beta}\delta_{\alpha'\beta'} - \sum_{\nu\nu'} \int_0^t dt' e^{i\mathcal{L}_{\alpha\alpha'}^0 t'} J_{\alpha\alpha'\nu\nu'}(e^{i\hat{\mathcal{L}}(t-t')})_{\nu\nu',\beta\beta'}, \quad (4)$$

where

$$e^{i\mathcal{L}_{\alpha\alpha'}^0 t} = e^{i\int_0^t dt' \omega_{\alpha\alpha'}(R_{\alpha\alpha'}, t)} e^{iL_{\alpha\alpha'} t} \equiv \mathcal{W}_{\alpha\alpha'}(0, t) e^{iL_{\alpha\alpha'} t}. \quad (5)$$

The solution of the integral equation may be found by iteration to yield a representation of the dynamics as a sequence of terms involving increasing numbers of non-adiabatic transitions.

A straightforward evaluation of the series solution may be obtained by a hybrid Monte Carlo–molecular dynamics (MC–MD) scheme where the possible quantum transitions, their number and the times at which they occur are sampled from suitable distributions [4, 12, 13]. While the iterated integral solution of the propagator provides an exact representation of quantum–classical dynamics in terms of surface-hopping trajectories and the hybrid MC–MD scheme has been implemented successfully for short times, it will fail for long times. Consequently, there is a need to develop more effective and efficient algorithms. In this paper we explore an alternative hybrid method to obtain a solution to the quantum–classical evolution equations which is more efficient and easier to implement than the hybrid scheme used in our earlier studies.

In section 2 we show how the quantum–classical propagator can be written in a sequence of short-time propagators. The evolution in the short time segments is given in terms of a discretization of the first-order truncation of the Dyson form of the propagator. We show that in the limit where the number of segments N goes to infinity and the segment length Δt goes to zero, with $N \Delta t = t$, we recover the full iterated form of the Dyson quantum–classical propagator for the time interval t . The section also contains a description of how the algorithm is implemented. Section 3 presents the results of simulations using this algorithm for the spin-boson system. Since exact numerical results are available for this model and quantum–classical simulations of the iterated full Dyson propagator have been carried out, we are able to assess the utility of the algorithm. The conclusions of the paper are presented in section 4.

2. Sequential short-time propagation

The simulation scheme that we develop in this paper utilizes the fact that the quantum–classical Liouville operator $\hat{\mathcal{L}}$ is time independent, so the evolution operator can be simply decomposed into a composition of evolution operators in time segments of arbitrary length. The evolution of a dynamical variable (or the density matrix) over any time interval can then be obtained by the successive application of evolution operators in small time intervals.

In order to present this method in compact form we adopt a notation for pairs of quantum states introduced earlier [13]. We associate an index $s = \alpha\mathcal{N} + \alpha'$ with the pair $(\alpha\alpha')$, where $0 \leq \alpha, \alpha' < \mathcal{N}$ for an \mathcal{N} -state quantum subsystem. Consider dividing the time interval t into N segments of lengths Δt_j such that the j th segment $t_j - t_{j-1} = \Delta t_j$. We may then write

$$(e^{i\mathcal{L}t})_{s_0 s_N} = \sum_{s_1 s_2 \dots s_{N-1}} \prod_{j=1}^N (e^{i\mathcal{L}(t_j - t_{j-1})})_{s_{j-1} s_j}. \quad (6)$$

Using this compact notation, the operator identity in equation (4),

$$(e^{i\hat{\mathcal{L}}(t_j - t_{j-1})})_{s_{j-1} s_j} = e^{i\mathcal{L}_{s_{j-1}}^0 (t_j - t_{j-1})} \delta_{s_{j-1} s_j} - \sum_{s_l} \int_{t_{j-1}}^{t_j} d\tau_1 e^{i\mathcal{L}_{s_j}^0 (\tau_1 - t_{j-1})} J_{s_{j-1} s_l} (e^{i\hat{\mathcal{L}}(t_j - \tau_1)})_{s_l s_j}, \quad (7)$$

holds in every time interval.

Various levels of approximation can be constructed by truncating the operator identity within each time slice. Here we suppose that the time intervals $t_j - t_{j-1} = \Delta t$ are sufficiently small that one may keep only the first term in the series solution obtained by iterating the integral Dyson equation (7). We have

$$(e^{i\hat{\mathcal{L}}(t_j - t_{j-1})})_{s_{j-1} s_j} = e^{i\mathcal{L}_{s_{j-1}}^0 (t_j - t_{j-1})} \delta_{s_{j-1} s_j} - \int_{t_{j-1}}^{t_j} d\tau_1 e^{i\mathcal{L}_{s_{j-1}}^0 (\tau_1 - t_{j-1})} J_{s_{j-1} s_j} e^{i\mathcal{L}_{s_j}^0 (t_j - \tau_1)}. \quad (8)$$

Since the time interval Δt is assumed to be sufficiently small, we can take a one-point approximation to the time integral by choosing a point t' in Δt :

$$(e^{i\hat{\mathcal{L}}(t_j-t_{j-1})})_{s_{j-1}s_j} \approx e^{i\mathcal{L}_{s_{j-1}}^0(t'-t_{j-1})}(\delta_{s_j s_{j-1}} - \Delta t J_{s_{j-1}s_j})e^{i\mathcal{L}_{s_{j-1}}^0(t_j-t')}. \quad (9)$$

In particular, by way of illustration, if we choose $t' = t_j$ we obtain

$$\begin{aligned} (e^{i\hat{\mathcal{L}}(t_j-t_{j-1})})_{s_{j-1}s_j} &\approx e^{i\mathcal{L}_{s_{j-1}}^0(t_j-t_{j-1})}(\delta_{s_j s_{j-1}} - \Delta t J_{s_{j-1}s_j}) \\ &= \mathcal{W}_{s_{j-1}}(t_{j-1}, t_j) e^{i\mathcal{L}_{s_{j-1}}^0(t_j-t_{j-1})}(\delta_{s_j s_{j-1}} - \Delta t J_{s_{j-1}s_j}). \end{aligned} \quad (10)$$

Thus, at the end of each small segment, the system either may remain in the same pair of adiabatic states or make a transition to a new pair of states. Substituting this expression into equation (6), we obtain

$$(e^{i\mathcal{L}t})_{s_0 s_N} \approx \sum_{s_1 s_2 \dots s_{N-1}} \prod_{j=1}^N e^{i\mathcal{L}_{s_{j-1}}^0(t_j-t_{j-1})}(\delta_{s_j s_{j-1}} - \Delta t J_{s_{j-1}s_j}). \quad (11)$$

Here and in the following $t_j = j \Delta t$ and $t_N = t$. In the limit $N \rightarrow \infty$, $\Delta t \rightarrow 0$ with $N \Delta t = t$, we recover the iterated form of the Dyson integral propagator. This may be seen by writing equation (11) explicitly to obtain

$$\begin{aligned} (e^{i\mathcal{L}t})_{s_0 s_N} &= e^{i\mathcal{L}_{s_0}^0 t} \delta_{s_0 s_N} + \sum_{n=1}^N (-1)^n \sum_{s_1, s_2, \dots, s_{n-1}} \sum_{k_1=1}^{N-n+1} \sum_{k_2=k_1+1}^{N-n+2} \dots \sum_{k_n=k_{n-1}+1}^N e^{i\mathcal{L}_{s_0}^0(t_{k_1}-t_0)} \\ &\quad \times (\Delta t J_{s_0 s_1}) e^{i\mathcal{L}_{s_1}^0(t_{k_2}-t_{k_1})} (\Delta t J_{s_1 s_2}) \dots (\Delta t J_{s_{n-1} s_N}) e^{i\mathcal{L}_{s_N}^0(t-t_{k_n})}. \end{aligned} \quad (12)$$

In this equation no sum over the s_i -indices is to be taken for $n = 1$. By inspection, it is evident that in the limit given above, equation (12) is the discretized version of the iterated form of the Dyson expression given in equation (7).

Now we can consider the calculation of the expectation value of an observable $\hat{O}_W(R, P, t)$:

$$\begin{aligned} \overline{O}(t) &= \sum_{s_0} \int dR dP O_W^{s_0}(R, P, t) \rho_W^{s'_0}(R, P) \\ &= \sum_{s_0, s_N} \int dR dP [(e^{i\mathcal{L}t})_{s_0 s_N} O_W^{s_N}(R, P)] \rho_W^{s'_0}(R, P) \\ &= \sum_{s_0, s_1, \dots, s_N} \int dR dP \left[\prod_{j=1}^N (e^{i\mathcal{L}(t_j-t_{j-1})})_{s_{j-1}s_j} \right] O_W^{s_N}(R, P) \rho_W^{s'_0}(R, P), \end{aligned} \quad (13)$$

where s'_0 is obtained from s_0 by the interchange $\alpha \rightleftharpoons \alpha'$ and $\rho_W^{s'_0}(R, P)$ is the initial value of the density matrix. The last line of equation (13) was obtained by inserting for the evolution operator the sequential propagation expression in equation (11).

To carry out the calculation, the multi-dimensional sums over quantum indices and integrals over phase-space variables may be evaluated through Monte Carlo sampling. We begin by choosing s_0 from the set \mathcal{S}_0 of permitted values for an \mathcal{N} -state system and note the weight $w_{s_0} = \mathcal{N}^2$. Next, we choose (R, P) from $|\rho_W^{s'_0}(R, P)|$ and note the sign, $\sigma(\rho)$, of $\rho_W^{s'_0}(R, P)$. To avoid the branching of trajectories induced by the successive application of the off-diagonal operator J , we utilize the momentum jump approximation introduced earlier [4].

To propagate the dynamics through one time interval, we update the initial positions and momenta, the phase factor and the observable at time Δt by applying $e^{i\mathcal{L}_{s_0} \Delta t}$. Then, given s_0 , we choose s_1 uniformly from the set \mathcal{S}_1 of allowed final states. The weight $w_{s_0 s_1}$ associated

with the final state is the number of elements of the set $N(S_1)$. Having chosen s_1 we can compute the non-adiabatic coupling matrix element d_{s_0, s_1} at the updated position.

To proceed, define the probability, Π , of a non-adiabatic transition:

$$\Pi = \left| \frac{P_{s_{I-1}, \Delta t}}{M} d_{s_{I-1}, s_I}(R_{s_{I-1}, \Delta t}) \right| \Delta t \left(1 + \left| \frac{P_{s_{I-1}, \Delta t}}{M} d_{s_{I-1}, s_I}(R_{s_{I-1}, \Delta t}) \right| \Delta t \right)^{-1}, \quad (14)$$

and sample from it:

(a) If the jump is rejected, then

$$O_W^{s_0}(R, P, \Delta t) = \mathcal{W}_{s_0}(R_{s_0, \Delta t}, \Delta t) O_W^{s_0}(R_{s_0, \Delta t}, P_{s_0, \Delta t}) \frac{1}{1 - \Pi}. \quad (15)$$

(b) If it is accepted, then, using the momentum jump approximation, we translate the momentum $P_{s_0, \Delta t}$ to (to avoid numerical instabilities associated with the momentum jump approximation, we have introduced an upper bound on the acceptable values of S , such that if $|S| > S_c$ the contribution of the trajectory to $\bar{O}(t)$ at that and all subsequent time slices is discarded)

$$P_{s_1, \Delta t} = P_{s_0, \Delta t} + \frac{1}{2} S_{s_0 s_1}$$

and we write

$$O_W^{s_1}(R, P, \Delta t) = \mathcal{W}_{s_0}(R_{s_0, \Delta t}) O_W^{s_0}(R_{s_0, \Delta t}, P_{s_1, \Delta t}) \frac{P_{s_0, \Delta t}}{M} d_{s_0 s_1}(R_{s_0, \Delta t}) \frac{1}{\Pi} w_{s_0 s_1}. \quad (16)$$

This procedure may now be reapplied to obtain the observable $O_W^{s_j}(R, P, j \Delta t)$ for subsequent time slices until the N th slice is reached. Finally, multiplying the observable by w_{s_0} and the sign of the density matrix, and averaging the resulting quantity over the sampled initial conditions, we obtain the statistical average.

3. Results for the spin-boson model

We have applied this scheme to evaluate the decay of the population in the spin-boson model [16, 17], a system for which exact results are available [18] and which has been previously simulated using the quantum–classical Liouville equation and surface-hopping methods [13]. This model describes a two-level system, with states $\{|\uparrow\rangle, |\downarrow\rangle\}$, bilinearly coupled to a harmonic bath of N oscillators with masses M_j and frequencies ω_j . The partially Wigner transformed spin-boson Hamiltonian that enters the quantum–classical Liouville equation is

$$\hat{H}_W = -\hbar \Omega \hat{\sigma}_x + \sum_{j=1}^N \left(\frac{P_j^2}{2M_j} + \frac{1}{2} M_j \omega_j^2 R_j^2 - c_j R_j \hat{\sigma}_z \right), \quad (17)$$

which depends on the classical phase-space coordinates (R, P) and the spin degrees of freedom. The σ_i are the Pauli spin matrices. The values of the parameters in this N -oscillator spin-boson model were taken from Makri and Thompson [18], $c_j = (\xi \hbar \omega_0 M_j)^{1/2} \omega_j$, $\omega_j = -\omega_c \ln(1 - j \omega_0 / \omega_c)$ where $\omega_0 = \omega_c (1 - \exp(-\omega_{max} / \omega_c)) / N$ and $j = 1, \dots, N$. This parameter choice models a bath with ohmic spectral density characterized by the Kondo parameter ξ and frequency ω_c . The parameter ω_{max} is a cut-off frequency. Further details of the model, along with the forms of the adiabatic states and non-adiabatic coupling matrix elements, can be found in [13].

The partially Wigner transformed density matrix is taken to be uncorrelated with the subsystem in state $|\uparrow\rangle$ and with the bath in internal thermal equilibrium:

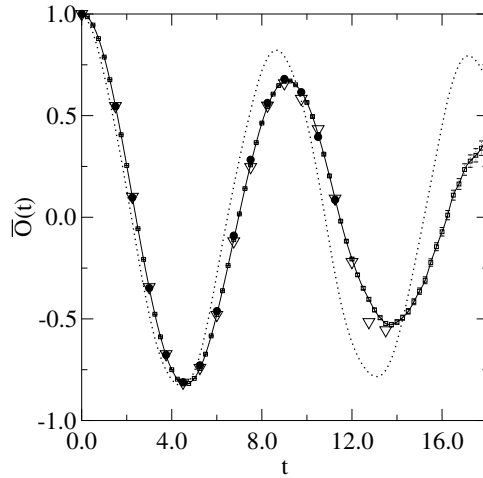


Figure 1. The time dependence of $\overline{O}(t)$ for $\xi = 0.007$, $\beta = 0.3/(\hbar\omega_c)$. Comparison of sequential short-time propagation (\square , broken curve), full Dyson solution (∇), influence functional theory (\bullet) and adiabatic dynamics (solid curve).

$$\hat{\rho}_W(R, P, 0) = \hat{\rho}_s(0)\rho_{bW}(R, P), \quad (18)$$

where, in dimensionless variables ($R'_j = (M_j\omega_c/\hbar)^{1/2}R_j$, $P'_j = (\hbar M_j\omega_c)^{-1/2}P_j$),

$$\rho_{bW}(R', P') = \prod_{i=1}^N \frac{\tanh(\beta\omega_i/2)}{\pi} \exp\left[-\frac{2 \tanh(\beta\omega_i/2)}{\omega_i} \left(\frac{P_i'^2}{2} + \frac{\omega_i^2 R_i'^2}{2}\right)\right]. \quad (19)$$

In order to compare our results, using the sequential short-time propagator, with earlier ones obtained using the exact Dyson propagator we focus our attention on the computation of the expectation value of the observable:

$$\hat{O} = \hat{\sigma}_z = \begin{pmatrix} 1 & 0 \\ 0 & -1 \end{pmatrix}, \quad (20)$$

whose average is the population difference in the quantum subsystem.

The system parameters used in this study were $\Omega = \omega_c/3$ and $\omega_{max} = 3\omega_c$, while the Kondo parameter and reduced temperature took the two sets of values ($\xi = 0.007$, $\beta = 0.3/(\hbar\omega_c)$) and ($\xi = 0.1$, $\beta = 3.0/(\hbar\omega_c)$). The harmonic bath consisted of ten oscillators. This choice of parameters allows one to explore non-adiabatic regimes at low and relatively high temperatures where the bath can be expected to become more ‘classical’, and weak to moderate coupling, where the dissipative effects of the bath become more evident.

Figure 1 plots the average value of the population difference of the two-state quantum subsystem versus time for $\xi = 0.007$ and $\beta = 0.3/(\hbar\omega_c)$. The sequential short-time propagation results are in very good agreement with the numerically exact results of Makri and Thompson [18] and with our earlier full Dyson solution. In contrast with a simple implementation of the full Dyson algorithm, the present scheme yields the entire time evolution of the observable with a single surface-hopping trajectory. The figure also presents the adiabatic evolution. Even for this small coupling strength one sees noticeable deviations from the exact quantum evolution, reflecting the importance of the non-adiabatic scheme for this problem.

An analogous set of results for a somewhat stronger coupling to the bath ($\xi = 0.1$, $\beta = 3.0/(\hbar\omega_c)$) is shown in figure 2. Equally good agreement is obtained in the time range

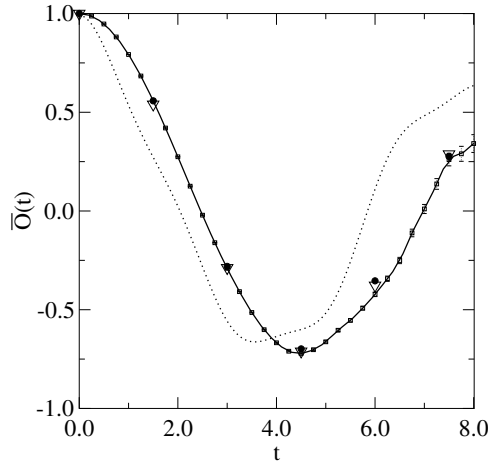


Figure 2. The time dependence of $\overline{O}(t)$ for $\xi = 0.1$, $\beta = 3/(\hbar\omega_c)$. Comparison of sequential short-time propagation (\square , broken curve), full Dyson solution (∇), influence functional theory (\bullet) and adiabatic dynamics (solid curve).

explored. In this case the stronger coupling to the bath manifests itself in the more non-harmonic character of the oscillations of the mean value of the observable and its more rapid decay to equilibrium. Note also that the adiabatic approximation to the dynamics fails badly in this case.

4. Conclusions

The short-time sequential propagation algorithm for the simulation of quantum–classical dynamics has been shown to provide a relatively simple scheme for the computation of dynamical properties. If this method is used in conjunction with the momentum jump approximation, once an initial phase-space point and pair of quantum states are chosen, each realization of the dynamics is a single stochastic trajectory. This trajectory comprises classical evolution segments punctuated by quantum transitions that change one of the quantum states in the pair and produce momentum changes in the classical environment. The classical evolution takes place on either single adiabatic potential energy surfaces if a diagonal pair of states is chosen in the quantum transition or on the mean of two adiabatic surfaces if the states in the chosen pair are distinct. The phase-space coordinates and quantum states may be recorded at times separated by intervals Δt along the trajectory. Once this trajectory is computed one may assemble all the information needed to compute the observable at all intermediate times between 0 and t in the history as described in the section devoted to the algorithm. In particular, the phase factors \mathcal{W}_{s_j} enter the computation for segments of the trajectory involving distinct pairs of states and reflect the quantum coherence that exists in the system.

The results of the calculations on the spin-boson model demonstrated that the algorithm can be used to simulate the quantum–classical dynamics of systems with many classical degrees of freedom. Since the complexity of the classical system simply determines the nature of the classical evolution segments, and one may exploit well-developed molecular dynamics methods to carry out these portions of the dynamics, the simplifications provided in the quantum–classical framework by the short-time sequential algorithm should allow one to treat realistic many-body systems of physical interest.

Acknowledgments

This work was supported in part by a grant from the Natural Sciences and Engineering Research Council of Canada and also by a MIUR COFIN 2000 project. Acknowledgement is made to the donors of The Petroleum Research Fund, administered by the ACS, for partial support of this research. RK would like to thank the Commissione Calcolo of INFN for supporting an extended visit to 'La Sapienza' where a large part of this work was carried out; DMK is grateful to CECAM for supporting a few short visits to Rome. We also acknowledge support from the European Science Foundation through the SIMU programme.

References

- [1] Kapral R and Ciccotti G 2002 *A Statistical Mechanical Theory of Quantum Dynamics in Classical Environments* ed M Mareschal and P Nielaba (Berlin: Springer)
- [2] Herman M F 1994 *Annu. Rev. Phys. Chem.* **45** 83
- [3] Tully J C 1998 *Modern Methods for Multidimensional Dynamics Computations in Chemistry* ed D L Thompson (New York: World Scientific) p 34
- [4] Kapral R and Ciccotti G 1999 *J. Chem. Phys.* **110** 8919
- [5] Tully J C 1990 *J. Chem. Phys.* **93** 1061
- [6] Tully J C 1991 *Int. J. Quantum Chem.* **25** 299
- [7] Hammes-Schiffer S and Tully J C 1994 *J. Chem. Phys.* **101** 4657
- [8] Sholl D S and Tully J C 1998 *J. Chem. Phys.* **109** 7702
- [9] Xiao L and Coker D F 1994 *J. Chem. Phys.* **100** 8646
- [10] Coker D F and Xiao L 1995 *J. Chem. Phys.* **102** 496
- [11] Mei H S and Coker D F 1996 *J. Chem. Phys.* **104** 4755
- [12] Webster F, Rossky P J and Friesner P A 1991 *Comput. Phys. Commun.* **63** 494
- [13] Webster F, Wang E T, Rossky P J and Friesner P A 1994 *J. Chem. Phys.* **100** 483
- [14] Martinez T J, Ben-Nun M and Levine R D 1997 *J. Phys. Chem. A* **101** 6389
- [15] Martens C C and Fang J-Y 1996 *J. Chem. Phys.* **106** 4918
- [16] Donoso A and Martens C C 1998 *J. Phys. Chem.* **102** 4291
- [17] Wan C and Schofield J 2000 *J. Chem. Phys.* **113** 7047
- [18] Santer M, Manthe U and Stock G 2001 *J. Chem. Phys.* **114** 2001
- [19] Nielsen S, Kapral R and Ciccotti G 2000 *J. Chem. Phys.* **112** 6543
- [20] Nielsen S, Kapral R and Ciccotti G 2000 *J. Stat. Phys.* **101** 225
- [21] MacKernan D, Ciccotti G and Kapral R 2002 *J. Chem. Phys.* **116** 2346
- [22] Nielsen S, Kapral R and Ciccotti G 2001 *J. Chem. Phys.* **115** 5805
- [23] Wigner E 1932 *Phys. Rev.* **40** 749
- [24] Leggett A J, Chakravarty S, Dorsey A T, Fisher M P A, Garg A and Zwerger M 1987 *Rev. Mod. Phys.* **59** 1
- [25] Weiss U 1999 *Quantum Dissipative Systems* (Singapore: World Scientific)
- [26] Thompson K and Makri N 1999 *J. Chem. Phys.* **110** 1343
- [27] Makri N 1999 *J. Phys. Chem. B* **103** 2823